 doi:10.20944/preprints202012.0608.v1

Article

Design and testing of mobile laboratory for mitigation of gaseous emissions from livestock agriculture with photocatalysis

Myeongseong Lee [1], Jacek A. Koziel [1,*], Wyatt Murphy [1], William S. Jenks [2], Blake Fonken [1], Ryan Storjohann [1], Baitong Chen [1], Peiyang Li [1], Chumki Banik [1], Landon Wahe [1], Heekwon Ahn [3]

[1] Department of Agricultural and Biosystems Engineering, Iowa State University, Ames, IA 50011, USA; leefame@iastate.edu (M.L.), koziel@iastate.edu (J.K.), wmurphy@iastate.edu (W.M.), bjfonken@iastate.edu (B.F.), rls1@iastate.edu (R.S.), baitongc@iastate.edu (B.C.), peiyangl@iastate.edu (P.L.), cbanik@iastate.edu (C.B.), lwahe@iastate.edu (L.W.)

[2] Department of Chemistry, Iowa State University, Ames, IA 50011, USA; wsjenks@iastate.edu (W.J.)

[3] Department of Animal Biosystems Sciences, Chungnam National University, Daejeon 34134, Korea; hkahn@cnu.ac.kr (H.A.)

* Correspondence: koziel@iastate.edu; Tel.: +1-515-294-4206

Abstract: Livestock production systems generate nuisance odor and gaseous emissions affecting local communities and regional air quality. Also, there are concerns about the occupational health and safety of farm workers. Proven mitigation technologies that are consistent with the socio-economic challenges of animal farming are needed. We have been scaling up the photocatalytic treatment of emissions from lab-scale, aiming at farm-scale readiness. In this paper, we present the design, testing, and commissioning of a mobile laboratory for on-farm research and demonstration of performance in real farm conditions. The mobile lab is capable of treating up to 1.2 $m^3 \cdot s^{-1}$ of air with TiO_2-based photocatalysis and adjustable UV-A dose based on LED lamps. We summarize the main technical requirements, constraints, approach, and performance metrics for the mobile laboratory, such as the effectiveness (measured as the percent reduction) and cost of photocatalytic treatment of air. The commissioning of all systems with standard gases resulted in ~9% and 34% reduction of NH_3 and butan-1-ol, respectively. We demonstrated that as the percent reduction of standard gases increased with increased light intensity and treatment time. These results show that the mobile laboratory was ready for on-farm deployment and evaluating the effectiveness of UV treatment.

Keywords: air pollution control, air quality, volatile organic compounds, odor, environmental technology, advanced oxidation, UV-A, titanium dioxide

1. Introduction

Over the past few decades, livestock and poultry farmers have adopted new technology and have scaled up farming operations to meet society's demand for high-quality meats, milk, eggs, and by-products. Large confined animal feeding operations (CAFOs) are common in many parts of the world. This has generated profits and jobs, but the environmental problems associated with the local air quality have been exacerbated. These unwanted side effects of animal production require sustainable solutions for the benefit of workers, rural communities, and the industry.

The U.S. National Air Emissions Monitoring Study (NAEMS) developed an accurate baseline emission database for CAFO regulation by the US EPA through the notification provisions of the Emergency Planning and Community Right-to-Know Act (EPCRA) and the Clean Air Act (CAA) [1,2]. NAEMS and the companion projects focused on monitoring emissions of odor, odorous VOCs, ammonia (NH_3), hydrogen sulfide (H_2S), carbon dioxide (CO_2), methane (CH_4), the total suspended particulates (TSP), PM10, and PM2.5 in the egg, broiler, dairy, and swine production industries [1-7]. While the NAEMS can be used as a standard and a source of the pollutants emitted from farms, there

 doi:10.20944/preprints202012.0608.v1

is still a need to develop and test mitigation technologies that are consistent with the socio-economic reality of CAFOs.

Farm-scale performance data are a prerequisite for the adoption of proposed new technology. Farmers need proven technologies before agreeing on farm-scale trials. Well-intentioned, laboratory-scale experimentation cannot fully duplicate the on-farm variability. Maurer et al. (2016) summarized the current state of adoption of technologies for mitigation of gaseous emissions from livestock agriculture [8]. Only ~25% of mitigation technologies developed and tested in lab-scale have been tested in real-farm conditions. We have been scaling up the photocatalytic treatment of emissions from the lab- to pilot-scales, aiming at farm-scale readiness [9-16].

UV light treatment is a promising technology for mitigating gaseous pollutants. The use of either shorter UV wavelengths or a photocatalyst improves the mitigation effects [11,13,14]. In addition, catalytic coating type, coating dose, UV dose, relative humidity, temperature, and dust accumulation (on photocatalyst) are important variables to consider and optimize for improved reduction of targeted odorous gases [11,16]. The photocatalytic treatment has been found to show a significant reduction in odorous VOCs even after short effective treatment times that are consistent with fast-moving ventilation air on farms [9,14]. Previous studies have reported the varying effect of reducing NH_3, H_2S, greenhouse gases, VOCs, odor, and PM with UV in livestock farm conditions [6,7,9-20].

Only a selected few studies reported on testing UV technology on a pilot scale [10,12,14] or farm-scale [17,18]. For that reason, there is a lack of information on UV doses and cost to reduce odorous gases in farm-scale conditions. Also, depending on the wavelengths of UV light, direct exposure to the light or its by-products (e.g., ozone) generated by shorter wavelength UV (e.g., 254 nm) can be risky to workers and livestock. Our previous research showed that the intrinsically safer UV-A (365 nm) could be effective in treating NH_3, N_2O, ozone, selected VOCs, and odor on lab- and pilot-scales [10-12].

Therefore, we hypothesize that the UV-A based photocatalysis can be effective in reducing selected gaseous emissions at a much larger scale. A UV-A mobile lab is a research tool that could be used to perform on-site trials at different farms and industrial emissions sources to demonstrate UV-A performance at realistic conditions. The farmers and industry appreciate these types of trials that do not disrupt current operations while providing necessary decision-making data. This was the motivation behind the design of a self-contained mobile laboratory that can directly sample the gases from a livestock farm and carry out the evaluation of photocatalysis UV treatment and cost prior to the next logical step, i.e., scaling up and installation of UV treatment on a farm or other emissions source.

The objective of this research was to design and test of mobile laboratory for mitigation of gaseous emission from livestock barns with UV-A photocatalysis. To our knowledge, this is the first study to evaluate the effect of UV-A photocatalysis treatment under conditions similar to a livestock farm using a mobile laboratory of this type. We summarize the main technical requirements, constraints, approach, and performance metrics for the mobile laboratory, such as the effectiveness (measured as the percent reduction) and cost of photocatalytic treatment of air. We provide the mitigation effect for two representative odorous gases (NH_3 and butan-1-ol) with the mobile laboratory. In addition, preliminary economic analysis for the cost of gaseous emissions treatment with LED UV-A lights was provided.

2. Materials and Methods

2.1 Requirements for testing UV photocatalysis at the mobile laboratory

The mobile laboratory (7.2 m × 2.4 m × 2.4 m exterior dimensions) was designed to evaluate the effectiveness of UV photocatalysis by directly connecting to the exhaust gases emitted from the farm (Figure 1).

Preprints (www.preprints.org) | NOT PEER-REVIEWED | Posted: 24 December 2020 doi:10.20944/preprints202012.0608.v1

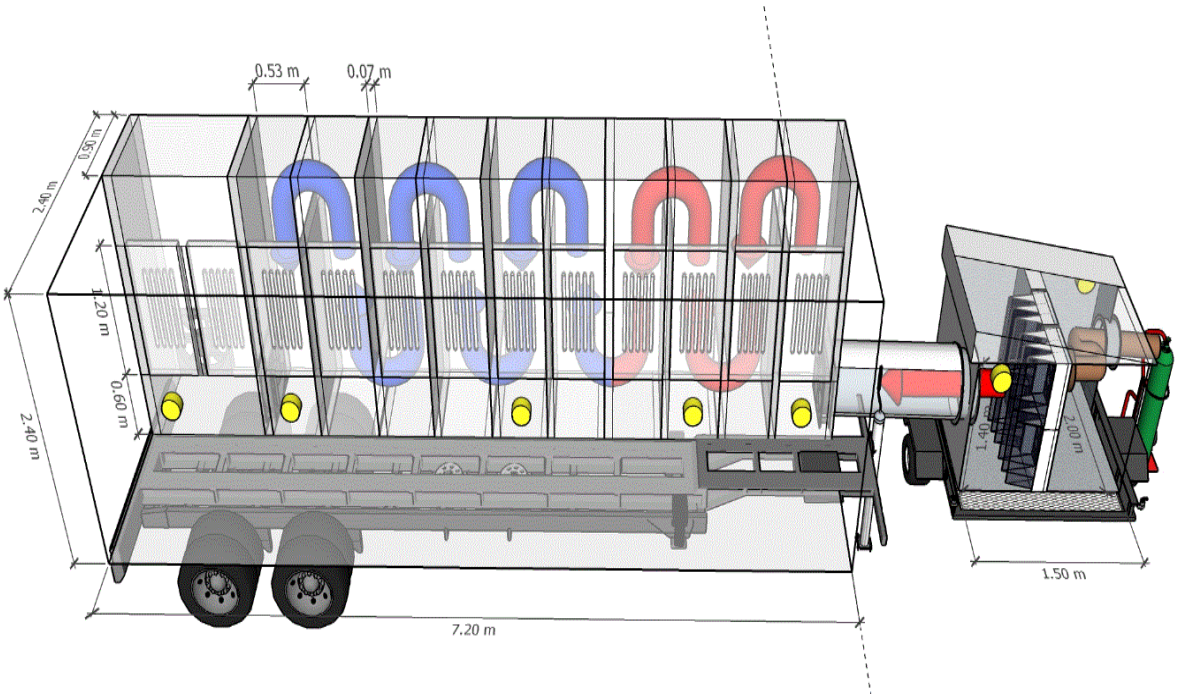

Figure 1. Schematic of a flow-through UV mobile laboratory with an upstream filtration unit. Brown arrow: inlet of untreated air; red arrow: inlet air with reduced particle matter load (after filtration); blue arrow: UV-treated air. The untreated air (brown arrow) could be either (a) standard gas (illustrated by the green compressed gas cylinder), (b) mixture of standard gases, (c) surrogate odorous air, (d) exhaust from livestock barn, or other air pollution source. Yellow: gas sampling ports used for evaluation of treatment efficiency.

The technical requirements and constraints for the mobile laboratory are summarized in Table 1. It explains the approach, the performance metric, and the location of the detailed description in the manuscript that addresses each of the five main requirements and constraints. In summary, we have implemented 1) Construction of treatment chambers capable of irradiating UV light and collecting real-time gas samples, 2) control of the UV dose, 3) control of the airflow, 4) control of the photocatalyst dose, and 5) control of airborne particulate matter.

Table 1. Requirements for the mobile laboratory to evaluate the effectiveness of UV photocatalysis at a farm-scale. SM = Supplementary Materials.

Requirement	Constraints	Approach	Performance Metric	Detailed Description
1) Mobile lab for on-site testing of UV treatment on gaseous emissions from livestock barns	Mobility	Repurposed mobile trailer	Can be towed on public roads	Figure 1 Figure A.1 SM 1
	The safe work environment for lab personnel to work on-site year-round	a) Space divided of UV treatment chamber and work area for samples b) Negative-pressure ventilation inside the UV treatment area c) Heating, air condition d) Airtight UV treatment chamber	a) Can be safely operated (e.g., collecting data) during UV treatment b) Maintaining room temperature inside the work	Figure 1 Figure A.6 Figure A.7 SM 1, 6, and 8

Preprints (www.preprints.org) | NOT PEER-REVIEWED | Posted: 24 December 2020 doi:10.20944/preprints202012.0608.v1

		e) Rodent-proof	area regardless of ambient air	
	Installation of coated FRP for photocatalytic reaction	Fixed the coated FRP to all surfaces of the UV chamber with a pushpin	Coated ~ 76% of the surface area in the one UV chamber	SM 1
	Connectivity to the air pollution source	Large (dia = 0.5 m) flexible ducting for easy connection to barn exhaust fans	Figure A.6 SM 1	SM 1
		Safe routing of the excess of fan exhaust	It cannot affect the barn fan performance	-
	'Plug-and-play' 110V power management for 50 Amp lab	30 m (grade type) cable with NEMA (type) plug	-	-
	Insufficient of the photocatalysis reaction surface with UV light and coated TiO_2	Constructed vertical baffles inside the UV treatment chamber	SM 1	SM 1
2) Control the UV dose (via lamps' power)	Insufficient number of installed lamps to increase the photocatalysis reaction	Installed additional UV lamp holders measuring UV irradiance	Can control UV dose (~5.8 $mJ \cdot cm^{-2}$, SM 3, 4, and 5)	Figure A.2 Figure A.4 SM 2
3) Control the volumetric airflow	Ability to treat ~0.25 to1.0 $m^3 \cdot s^{-1}$ of air	a) Installed two fans and 1 anemometer fan b) Built a monitor system to see the volumetric flow rate measured by the anemometer fan	Can control airflow from ~0.25 $m^3 \cdot s^{-1}$ (535 CFM) to ~1.23 $m^3 \cdot s^{-1}$ (2,600 CFM).	SM 6 and 8
4) Control the photocatalyst dose	The necessity of coating method for the TiO_2 on the FPR surface	Coated through precise spray control	Material and Method 2.4	Discussion 4.2 Appendix B
5) Control airborne particulate matter	The necessity to remove airborne substances from the incoming gases for accurately investigating the reduction effect of photocatalysis	Installed the MERV filtration unit	SM 7	Figure A.5 SM 7

FRP = fiberglass reinforced plastic; MERV = minimum efficiency reporting value.

Preprints (www.preprints.org) | NOT PEER-REVIEWED | Posted: 24 December 2020 doi:10.20944/preprints202012.0608.v1

2.2 Light intensity measurement

Light intensity was measured (Figure A.3) with an ILT-1700 radiometer (International Light Technologies, Peabody, MA, USA) equipped with an NS365 filter and SED033 detector (International Light Technologies, Peabody, MA, USA). Prior to use, the radiometer and sensor were sent to the manufacturer company (International Light Technologies, Peabody, MA, USA) for factory calibration. For economic analysis, the electric power consumption was measured using a wattage meter (P3, Lexington, NY, USA).

2.3 Measurement of standard gases concentration (NH_3 and butan-1-ol)

Two odorous gases were used for testing and commissioning. The butan-1-ol (model for VOCs) and NH_3 concentrations were measured in order to evaluate the percent reduction by UV photocatalysis treatment (Figure 2). The calibrations for both standard gases were at $R^2 > 0.99$.

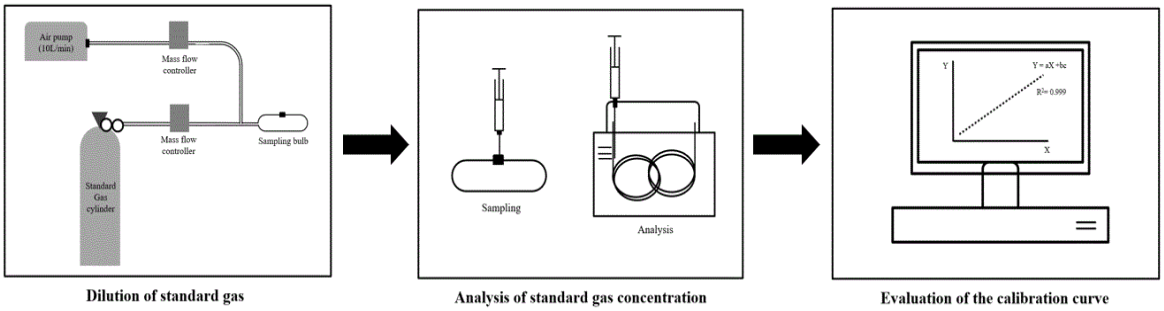

Figure 2. Calibration method for measuring targeted gas concentration. (1) Five standard gas concentrations were prepared/diluted to be within the range of the target gas to be measured. (2) Standard gas samples were analyzed with SPME-GC-MS or electrochemical gas sensors resulting in a gas concentration calibration curve.

For NH_3, standard gas and dry air were adjusted using a mass flow controller (FMA5400A/5500A Series, OMEGA, Norwalk, USA) to make five diluted gas samples generally within the range of the target gas to be measured. In the case of NH_3, diluted samples were collected in a Tedlar bag, and the concentration was measured using the gas monitoring system (OMS-300, Smart Control & Sensing Inc., Daejeon, Rep. of Korea) equipped with electrochemical gas sensors of Membrapor Co. (Wallisellen, Switzerland). The calibration curve is drawn using the obtained voltage from the sensor and the known concentration of the diluted sample (Figure 3).

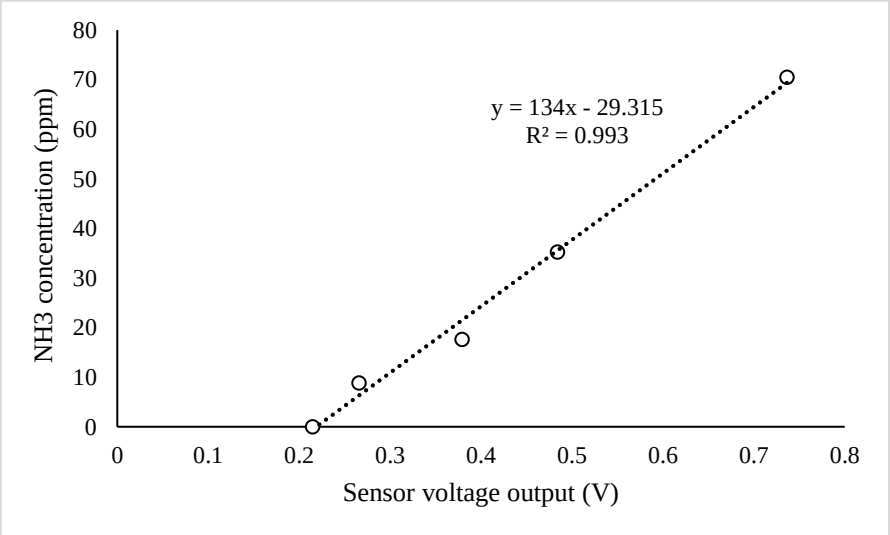

Figure 3. Calibration for real-time NH_3 measurements.

Preprints (www.preprints.org) | NOT PEER-REVIEWED | Posted: 24 December 2020 doi:10.20944/preprints202012.0608.v1

Air samples for butan-1-ol measurements were collected using 1 L glass gas sampling bulbs (Supelco, Bellefonte, PA, USA). Air samples were taken using a portable vacuum sampling pump (Leland Legacy; SKC Inc., Eighty-Four, PA, USA) with a set flow rate of 5 L·min^{-1} for 3 min. Chemical analyses were completed using a solid-phase microextraction (SPME) (50/30 µm DVB/CAR/PDMS; 2 cm-long fibers, Supelco, Bellefonte, PA, USA) using static extraction for 1 h at room temperature and gas chromatography-mass spectrometry (GC-MS) system for analyses (Agilent 6890 GC; Microanalytics, Round Rock, TX, USA). The calibration for butan-1-ol is shown in Figure 4.

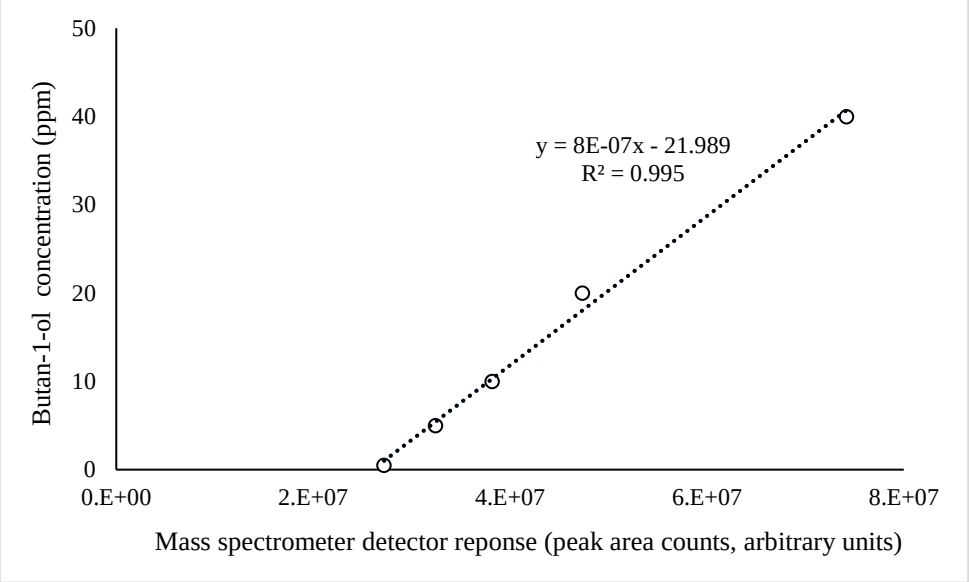

Figure 4. Calibration for butan-1-ol measurements.

2.4 Photocatalyst (TiO_2) coating

TiO2 coating was applied in the same way as in the previous study [10]. TiO2 coating on the pre-cut panels for the UV reactor was carried out based on an application protocol provided by PureTi (Cincinnati, OH, USA). In addition, training was provided by SATA (Spring Valley, MN, USA) for accurate spraying control. The temperature (25 °C) and relative humidity (40-45%) were adjusted to prevent instant evaporation of the sprayed TiO_2 solution (nanostructured anatase 10 µg·cm^{-2} TiO_2, PureTi, Cincinnati, OH, USA) before application. After cleaning the surface of the panel, the TiO_2 solution was sprayed. The spray pressure was adjusted to 60 psi with a regulator from the compressor, and the distance between the panel and the spray was ~0.15 m (6 in) at an angle of 90 deg. Coated panels were dried at room temperature for 3 days.

2.5 SEM-EDS analysis of photocatalyst coating and surfaces

The photocatalytic coating was analyzed to analyze the morphology and chemical composition on the surface of common building materials used for livestock barn interiors. Passive treatment of indoor air inside livestock facilities is the ultimate goal for UV treatment. Thus, the surface analyses of how the TiO2 coating interacts with common building materials is important, as the mitigation of emissions is, in part, driven by the photocatalyst integrity and uniformity. The scanning electron microscopy - energy-dispersive X-ray spectroscopy (SEM-EDS) analyses were performed at the Materials Analysis and Research Lab, Iowa State University. The SEM-EDS analysis was performed to analyze the TiO_2 coating morphology on the photocatalyst-coated surfaces. Samples coated TiO_2 were additionally coated with 2 nm iridium for conductivity and were lightly sprayed with canned air to remove loose dust particles before starting the analysis of SEM-EDS. The samples were examined in an FEI Quanta-FEG 250™ SEM at 10 kV. A range of magnifications was used. The samples used the electrons (S.E.) imaging and analyzed them in a high vacuum mode for improved resolution. Energy Dispersive Spectroscopy (EDS) analysis was done using an Oxford Instruments Aztec energy-dispersive

Preprints (www.preprints.org) | NOT PEER-REVIEWED | Posted: 24 December 2020 doi:10.20944/preprints202012.0608.v1

spectrometer with an X-Max 80 light-element detector (80 mm^2 active areas) for elemental and chemical analysis of a sample surface. A beam current of ~0.5 nA was used to generate an X-ray count rate of about 15k cps. X-ray maps of 256 × 244 pixels were collected for 10 min to show the distribution of the elements. That also produced a "sum" spectrum showing the overall X-ray signal from the field of view.

In addition, samples used in the previous study [11] were analyzed to compare whether there is a difference according to the material coated with the TiO_2 photocatalyst. For the TiO_2 sample coated on the glass used in the previous lab-scale study, samples on the glass were imaged with backscattered electrons (BSE) for which the brightness of the signal correlates with the density/average atomic number of the material for checking the TiO_2 coating morphology according to the material coated with TiO_2. In addition, samples were analyzed in variable pressure mode, where 60-100 Pa of water vapor was introduced into the chamber to dissipate the charge. Through this analysis, it was possible to confirm the chemical composition, arrangement, and morphology of the TiO_2-coated sample surface.

2.6 Data analysis – effectiveness and cost of photocatalytic treatment of air

The overall mean percent reduction for each measured gas was estimated as:

$$\%\ R = \frac{C_{con} - C_{Treat}}{C_{con}} \times 100 \quad (1)$$

Where: %R = percent reduction in gas concentrations during UV treatment.
C_{Con} & C_{Treat} = the mean measured concentrations in control and treated air, respectively.

Measured gas concentrations were adjusted to standard conditions (defined as 1 atm, 273.15 K) and dry air using collected environmental data:

$$C = \frac{C'}{(1-W)} \times \frac{P \cdot MW}{R \cdot T} \quad (2)$$

Where: C = a standard dry concentration of measured gas ($g \cdot m^{-3}$).
C' = the mean measured gas concentration in control and treated air ($mL \cdot m^{-3}$).
W = humidity ratio was calculated with Eq. 4 [1,21,22].
MW = molecular weight of target gas ($g \cdot mol^{-1}$).
R = 0.082057 $L \cdot atm \cdot mol^{-1} \cdot K^{-1}$.
T = measured air temperature (K).
P = measured pressure (atm).

The measured treated airflow rate was also adjusted to standard dry conditions at both control and treatment sampling locations:

$$Q = Q' \times (1 - W) \times \frac{P' \times 273.15}{P \times T} \quad (3)$$

Where: Q = dry standard airflow rate ($m^3 \cdot min^{-1}$).
Q' = actual measured (humid) airflow rate ($m^3 \cdot min^{-1}$).
W = humidity ratio calculated with Eq. 4 [21,22].
P'= actual pressure at the sampling point (atm).
P = standard pressure (atm).

The humidity ratio was estimated as:

$$W = 0.62198 \times \frac{e^{f(T)}\varphi}{(P_S \times 101325) - e^{f(T)}\varphi} \quad (4)$$

Where: W = humidity ratio (kg of water per kg of dry air).
Ps = pressure at the sampling location (atm).
φ = relative humidity (decimal).

For cases where T < 273.15 K [21,22]:

Preprints (www.preprints.org) | NOT PEER-REVIEWED | Posted: 24 December 2020 doi:10.20944/preprints202012.0608.v1

$$f(T) = \frac{c_1}{T} + c_2 + c_3T + c_4T^2 + c_5T^3 + c_6T^4 + c_7lnT$$

For cases where T > 273.16 K [21,22]:

$$f(T) = \frac{c_8}{T} + c_9 + c_{10}T + c_{11}T^2 + c_{12}T^3 + c_{13}lnT$$

Where: C_1 = -5.565·10^3, C_2 = 6.392, C_3 = -9.678·10^{-3}, C_4 = 6.222·10^{-7}, C_5 = 2.075·10^{-9}, C_6 = -9.484·10^{-13}, C_7 = 4.163, C_8 = -5.800·10^3, C_9 = 1.391, C_{10} = -4.864·10^{-2}, C_{11} = 4.176·10^{-5}, C_{12} = -1.445·10^{-8}, and C_{13} = 6.545.

Gas emissions were calculated as a product of measured gas concentrations and the total airflow rate:

$$E = (C \times Q) \quad (5)$$

Where: E = gas emissions (g·min^{-1}) of a target pollutant.

C = the mean measured target pollutant gas concentration in control or treated standard dry air (g·m^{-3}).

Q = dry standard airflow rate (m^3·min^{-1}).

The electric energy consumption was calculated using the measured power consumption of UV lamps during treatment. Electric energy consumption (kWh) during treatment was calculated using:

$$EEC = P \times t_s \times 3600^{-1} \times 10^{-3} \quad (6)$$

Where: EEC = electric energy consumption (kWh).

P = measured electric power consumption for the UV lamps turned 'on' during treatment (W).

t_s = treatment time for air in contact with the UV lamps that were turned 'on' inside the mobile lab (s).

The mass of mitigated gas pollutant (M) with UV during given treatment time (ts) was estimated by comparing gas emission rate (E) in treatment and control:

$$M = (E_{con} - E_{treat}) \times t_s \times 60^{-1} \quad (7)$$

Where: M = mass of mitigated gas pollutant (g).

E_{con} = emission rate at the 'control' sampling location.

E_{treat} = emission rate at the 'treatment' sampling location.

The electric energy of UV treatment (EE, kWh·g^{-1}) was estimated as using electric energy consumption (EEC) needed to mitigate a gas pollutant mass (M):

$$EE = \frac{EEC}{M} \quad (8)$$

Finally, the estimated cost of electric energy (Cost) needed for UV treatment was estimated using the mean cost ($·kWh^{-1}) of rural energy in Iowa ($0.13 kWh^{-1}, [23]):

$$Cost = EE \times \$0.13\ (\text{kWh})^{-1} \quad (9)$$

Where: Cost = estimated cost of electric energy needed for UV treatment to mitigate a unit mass of pollutants in the air ($·g^{-1}).

UV dose was estimated using measured light intensity (I) at a specific UV wavelength (mW·cm^{-2}) and treatment time (t_s). Since the photocatalysis reaction is assumed to be the main mechanism for the target gas mitigation, the light intensity irradiated on the TiO_2 surface was used.

$$UV\ dose = I \times t_s \quad (10)$$

Where: UV Dose = energy of the UV light on the surface of photocatalyst (mJ·cm^{-2}),

2.7 Statistical analysis

The program of R (version 3.6.2) was used to analyze the mitigation of target standard gases under the UV-A photocatalysis treatment. The mitigation depending on parameters of UV dose and treatment time between control concentration and treatment concentration was statistically analyzed

Preprints (www.preprints.org) | NOT PEER-REVIEWED | Posted: 24 December 2020 doi:10.20944/preprints202012.0608.v1

using one-way ANOVA. The statistical difference was confirmed by obtaining the p-value through the Tukey test. A significant difference was defined for a p-value <0.05 in this study.

3. Results

Testing UV-A treatment performance with two model standard gases (NH_3 and butan-1-ol) was essential during the mobile lab commissioning. Results are summarized below.

3.1 NH_3 percent reduction in treated air – effect of UV-A dose controlled by treatment time

The NH_3 percent reduction (%R) was investigated by increasing the UV dose by controlling the treatment time (Table 2). A 5% NH_3 standard gas was injected into the filtration unit inlet (Figure 1) and mixed with ambient air resulting in 67.8 ± 0.2 ppm at the inlet to the mobile laboratory. Initial testing used 60 UV lamps installed in 12 chambers (Figure 1); the NH_3 reduction was investigated by sampling at 3 different treatment times (from 29 to 57 s). The was no significant reduction in NH_3 with the largest UV dose tested (2.2 mJ·cm^{-2}). However, the measured concentrations in the control and treatment were reproducible. This observation led us to explore increasing the UV dose by installing additional UV lamps.

Table 2. Mitigation of NH_3 concentration under UV-A photocatalysis with 60 lamps (2.2 mJ·cm^{-2}). Control (Chamber #1, chamber nearest to the air inlet), C#6, C#10, C#12 (chamber nearest to the air outlet) signifies the location of air sampling ports. Airflow = 0.25 m^3·s^{-1}, inlet air temperature = 8 ℃, outlet air temperature = 9 ℃, RH = 39% (inside mobile laboratory). All (60) LED lamps were 'on'.

	Control	Chamber number (Treatment time, UV Dose)		
		C#6 (29 s, 1.2 mJ·cm^{-2})	C#10 (48 s, 1.9 mJ·cm^{-2})	C#12 (57 s, 2.2 mJ·cm^{-2})
NH_3 concentration (ppm)	67.9	67.9	67.4	67.5
	67.6	68.0	67.0	67.0
	67.8	67.6	65.0	63.8
Average ± S.D. (p-value)	67.8 ± 0.2	67.8 ± 0.2 (0.79)	66.5 ± 1.3 (0.23)	66.1 ± 2.0 (0.29)

3.2 NH_3 percent reduction in treated air – effect of UV-A dose controlled by light intensity and time

The NH_3 percent reduction (%R) was investigated by increasing the UV dose by installing additional lamps (from 60 to a total of 160) and maximizing treatment time (Table 3). The additional LED UV-A lamps (110 lamps) using portable UV lamp holders were installed in two chambers (#2 and #3) (Figure 1), and then the number of lamps turn 'on' was controlled.

A statistically significant reduction of 9-11% was measured (Table 3) for UV doses of 3.90 and 5.81 mJ·cm^{-2}. The extrapolated cost for removing 1 kg of NH_3 from the air was ~$53-$63. Furthermore, the high light intensity and shorter treatment time were more cost-effective compared with low light intensity and higher residence time.

Preprints (www.preprints.org) | NOT PEER-REVIEWED | Posted: 24 December 2020 doi:10.20944/preprints202012.0608.v1

Table 3. Mitigation of NH_3 with increasing UV-A light intensity and time. Airflow = 0.25 $m^3 \cdot s^{-1}$, temperature= 11 ± 3 ℃, RH = 34 ± 6%.

UV dose, $mJ \cdot cm^{-2}$ (# lamps [a], treatment time, t_s)	Measured gas concentration (ppm)		%R [b] (*p*-value)	Pollutant emission (*E*, $g \cdot min^{-1}$)		Power [c] (W)	Electric energy for mitigation of pollutant mass [d] (*EE*, $kWh \cdot g^{-1}$)	Cost ($\$ \cdot g^{-1}$) [e]
	Control	Treatment		Control	Treatment			
0.38 (10, 9.5 s)	67.8 ± 0.17	67.8 ± 0.21	0% (0.79)	0.76	0.76	160	Not estimated	Not estimated
0.67 (40, 9.5 s)	67.4 ± 0.35	67.4 ± 0.42	0% (0.93)	0.74	0.74	470	Not estimated	Not estimated
1.33 (60, 9.5 s)	67.6 ± 0.69	67.4 ± 0.35	0% (0.41)	0.74	0.74	790	Not estimated	Not estimated
2.48 (80, 9.5 s)	67.6 ± 0.32	66.9 ± 0.82	1% (0.36)	0.76	0.74	1,260	Not estimated	Not estimated
3.90 (110, 9.5 s**)**	**67.4 ± 0.36**	**61.1 ± 0.30**	**9% (<0.01)**	**0.75**	**0.68**	**1,730**	**0.41**	**0.05**
5.81 (160, 57 s**)**	**68.9 ± 0.68**	**61.1 ± 0.70**	**11% (<0.01)**	**0.76**	**0.68**	**2,500**	**0.48**	**0.06**

[a] The number of lamps turned 'on' during treatment; [b] percent reduction in gas concentrations; [c] measured electric power consumption for the UV lamps turned 'on' during treatment (W); [d] The electric energy of UV treatment (EE) estimated as using the electric energy consumption (EEC) needed to mitigate a gas pollutant mass (M) ($kWh \cdot g^{-1}$); [e] The cost of electric energy needed for UV treatment to mitigate a unit mass of pollutant in the air ($\$ \cdot g^{-1}$); **Bold** font signifies the statistical significance of treatment.

Measurement of NH_3 concentration after UV treatment was repeated three times with rapid 'lamps on' & 'lamps off' showing similar mitigation effects (Figure 5). This finding has practical significance because of the simplicity of activating treatment with no apparent lagtime.

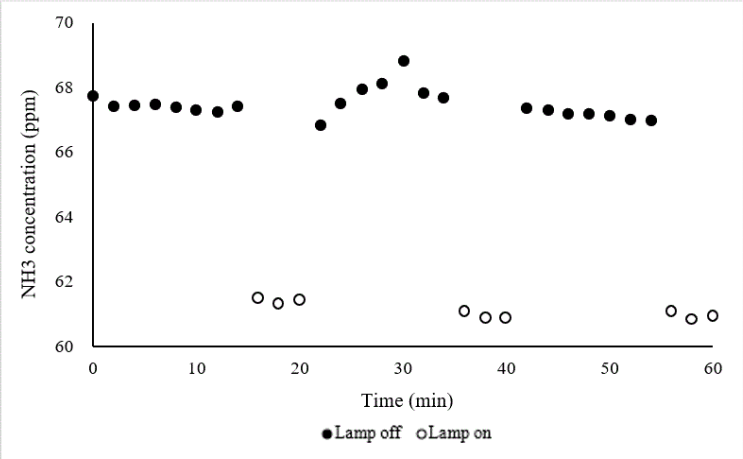

Figure 5. Mitigation of NH_3 concentration with 110 UV-A lamps inside the two chambers (#2 and #3, Figure 1). NH_3 concentration was measured at the effluent of chamber #3. Airflow = 0.25 $m^3 \cdot s^{-1}$, inlet air temperature (influent of chamber #2) = 13 ℃, outlet air temperature = 19 ℃, RH = 36% (effluent of chamber #3).

Preprints (www.preprints.org) | NOT PEER-REVIEWED | Posted: 24 December 2020 doi:10.20944/preprints202012.0608.v1

3.3 Butan-1-ol percent reduction in treated air – effect of UV-A dose controlled by treatment time

As with NH_3, there was no significant percent reduction for the initial 60 lamps turned on in 12 chambers (Table 4). A 100 ppm butan-1-ol standard gas was injected into the filtration unit inlet (Figure 1) and mixed with ambient air resulting in 0.63 ± 0.04 ppm at the inlet to the mobile laboratory and similar concentrations after UV treatment. Still, the measured concentrations in the control and treatment were reproducible. This observation led us to explore increasing the UV dose by installing additional UV lamps for this model VOC.

Table 4. Mitigation of butan-1-ol concentration under UV-A photocatalysis with 60 lamps. Control (Chamber #1, chamber nearest to the air inlet), C#6, C#10, C#12 (chamber nearest to the air outlet) signifies the location of air sampling ports. Airflow = 0.25 $m^3 \cdot s^{-1}$, inlet air temperature = 11 ℃, outlet air temperature = 13 ℃, RH = 34% (inside mobile laboratory). All (60) LED UVA lamps were 'on'.

	Control	Chamber number (Treatment time, UV Dose)		
	ppm	C#6 (29 s, 1.2 $mJ \cdot cm^{-2}$)	C#10 (48 s, 1.9 $mJ \cdot cm^{-2}$)	C#12 (57 s, 2.2 $mJ \cdot cm^{-2}$)
butan-1-ol (ppm)	0.59	0.55	0.62	0.63
	0.67	0.66	0.61	0.62
	0.62	0.66	0.63	0.69
Average ± S.D. (p-value)	0.63 ± 0.04	0.62 ± 0.06 (0.73)	0.62 ± 0.01 (0.87)	0.65 ± 0.04 (0.63)

3.5 Butan-1-ol percent reduction in treated air – effect of UV-A dose controlled by light intensity and time

A statistically significant percent reduction (19-41%) in butan-1-ol was found for the UV doses greater than 2.48 $mJ \cdot cm^{-2}$ (i.e., when additional lamps were installed, Table 5). The percent reduction for butan-1-ol was higher than NH_3. The percent reduction increased with the UV dose, but the 3.90 $mJ \cdot cm^{-2}$ appeared to be the most economically efficient (i.e., ~$0.35 to remove/mitigate 1 mg butan-1-ol from the air).

Table 5. Mitigation of butan-1-ol concentration with increasing light intensity. Airflow = 0.25 $m^3 \cdot s^{-1}$, temperature = 14 ± 2 ℃, RH = 34 ± 6%.

UV dose $mJ \cdot cm^{-2}$ **(# lamps [a], treatment time,** t_s**)**	**Measured gas concentration (ppm)**		***%R*** **[b] (*p*-value)**	**Pollutant emission (*E*, mg·min^{-1})**		**Power [c] (W)**	**Electric energy for mitigation of pollutant mass [d] (*EE*, kWh·mg^{-1})**	***Cost*** **($·mg^{-1}) [e]**
	Control	**Treatment**		**Control**	**Treatment**			
0.38 (10, 9.5 s)	0.63 ± 0.04	0.62 ± 0.63	0% (0.73)	29.9	29.5	160	Not estimated	Not estimated
0.67 (40, 9.5 s)	0.81 ± 0.27	0.67 ± 0.09	16% (0.33)	38.5	32.1	470	Not estimated	Not estimated
1.33 (60, 9.5 s)	0.67 ± 0.09	0.60 ± 0.03	10% (0.41)	32.1	28.6	790	Not estimated	Not estimated

Preprints (www.preprints.org) | NOT PEER-REVIEWED | Posted: 24 December 2020 doi:10.20944/preprints202012.0608.v1

2.48 (80, 9.5 s)	**0.66 ± 0.02**	**0.53 ± 0.06**	**19% (0.04)**	**31.5**	**25.3**	**1260**	**3.40**	**0.44**
3.90 (110, 9.5 s)	**0.65 ± 0.03**	**0.43 ± 0.04**	**34% (0.03)**	**30.9**	**20.3**	**1730**	**2.71**	**0.35**
5.81 (160, 57 s)	**0.69 ± 0.02**	**0.41 ± 0.07**	**41% (0.02)**	**32.9**	**19.4**	**2500**	**3.10**	**0.40**

[a] The number of lamps turned 'on' during treatment; [b] percent reduction in gas concentrations; [c] measured electric power consumption for the UV lamps turned 'on' during treatment (W); [d] The electric energy of UV treatment (EE) estimated as using the electric energy consumption (EEC) needed to mitigate a gas pollutant mass (M) (kWh·g^{-1}); [e] The cost of electric energy needed for UV treatment to mitigate a unit mass of pollutant in the air ($·g^{-1}); **Bold** font signifies the statistical significance of treatment.

Measurement of butan-1-ol concentration after UV treatment was repeated three times with rapid 'lamps on' & 'lamps off' showing similar mitigation effects (Figure 6) similarly to the effect observed for NH_3. This finding has practical significance because of the simplicity of activating treatment with no apparent lagtime.

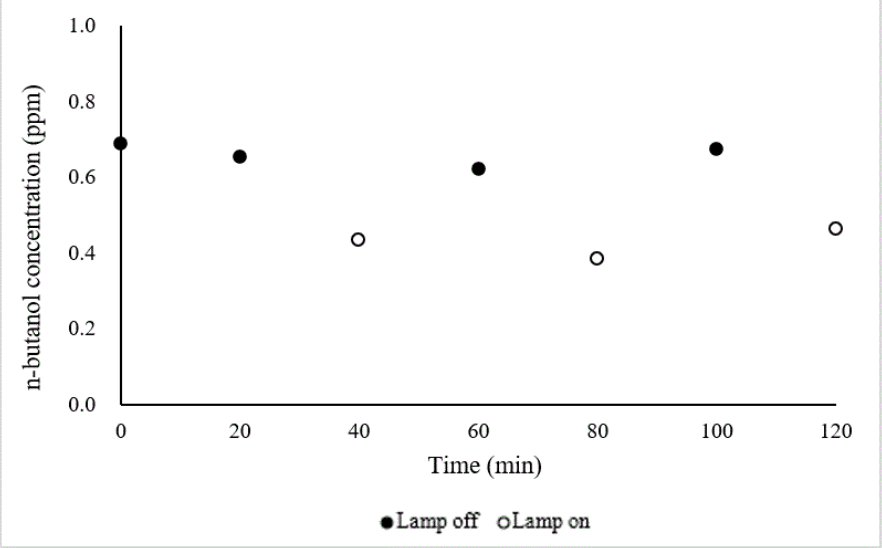

Figure 6. Mitigation of butan-1-ol (a.k.a. n-butanol) concentration with 110 UV-A lamps in the two chambers (#2 and #3). The reduction was measurement by adding UV-A lamps inside two chambers. Black means for light off, and white means for light on. Airflow = 0.25 m^3·s^{-1}, inlet air temperature = 13 °C, outlet air temperature = 19 °C, RH = 36% (inside mobile laboratory).

4. Discussion

4.1 Evaluation of TiO_2-based UV-A photocatalysis

Previous research on the mitigation of selected target gases via photocatalysis with UV-A in livestock-relevant environmental conditions was summarized in Table 6. In the case of NH_3, the photocatalysis showed a percent reduction from 7% ~ 19% as the light intensity increased in the lab-scale experiment [11]. At the pilot-scale [10], the reduction with photocatalysis efficiency was reduced to ~5% to 9%. Although the detailed mechanism of photocatalysis varies with different target pollutants, it is commonly agreed that the primary reactions responsible are interfacial redox reactions of the electron (e−) and hole (h+) on the surface of the photocatalyst coating material.

Preprints (www.preprints.org) | NOT PEER-REVIEWED | Posted: 24 December 2020 doi:10.20944/preprints202012.0608.v1

Therefore, this is considered that inhibiting factors, such as dust and high humidity, can reduce the interfacial redox reactions on the TiO_2 surface. In this study, a 9% reduction was observed when the average photocatalysis of light intensity at the photocatalytic surfaces was 0.49 $mW \cdot cm^{-2}$. Statistically significant NH_3 reduction was observed for sufficiently high light intensity even at shorter treatment times (9.5 s).

Table 6. Summary of percent reduction for NH_3 and VOCs with TiO_2 (coating thickness: 10 $\mu g \cdot cm^{-2}$) and UV-A light.

Reference	Experiment conditions	Treatment time[c] (s)	Light intensity ($mW \cdot cm^{-2}$)	Average percent reduction of target gas	
				NH_3 (range)	VOCs (range)
[16]	Lab-scale Temp[a]: 40 RH[b]: 40%	40, 200	0.06	Not reported	**DMDS (35.0 - 40.4)** **DEDS (27.7 - 81.0)** **DMTS (37.1 - 76.3)** **BA (62.2 - 86.9)** **Guaiacol (37.4 - 100.0)** **p-Cresol (27.4 - 93.8)**
[11]	Lab-scale Temp[a]: 25 ± 3 RH[b]: 12%	40, 200	0.44	**7.3 - 9.4**	Not reported
		40, 200	4.85	**10.4 - 18.7**	Not reported
[12]	Pilot-scale Temp[a]: 22~26 RH[b]: 36~80%	24, 47	< 0.04	Not reported	**AA (-52.9** to -19.7**)** **p-Cresol (**-21.4 - **22.0)**
[10]	Pilot-scale Temp[a]: 28 ± 3 RH[b]: 56%	100, 170	0.44	-0.2 - **5.2**	DEDS (12.7 - 18.7) BA (6.1 - 21.8) **p-Cresol** (**32.2** - 11.1) Skatole (-35.9 - 18.5)
		40, 170	4.85	2.5 - **8.7**	**DEDS** (18.1 - **47.2)** **BA** (22.1 - **61.9)** **p-Cresol** (21.8 - **49.3)** **Skatole** (53.6 - **35.4)**
This study	Pilot-scale Temp[a]: 19 RH[b]: 36%	9.5	Photolysis[d]: Ave 0.88 Photocatalysis[e]: Ave 0.49	**9.4**	**Butan-1-ol (34.4)**

[a] Temperature; [b] Relative humidity; [c] Time to irradiate the target gas with UV-A light; [d] Average of photolysis light intensity measured at three locations (top, middle, bottom); [e] Average of photocatalysis light intensity measured at eleven panels; dimethyl disulfide (DMDS), diethyl disulfide (DEDS), dimethyl trisulfide (DMTS), acetic acid (AA), butanoic acid (BA); **Bold** font signifies a statistical difference in mitigating gases with UV at ($p<0.05$).

Depending on the type of VOC, the reduction efficiency varied greatly. It means there was a significant decrease (mitigation) and increase (generation) in some types of VOC. VOCs also showed a higher percent reduction in lab-scale [11,16] experiments compared with the pilot-scale [10]. The

Preprints (www.preprints.org) | NOT PEER-REVIEWED | Posted: 24 December 2020 doi:10.20944/preprints202012.0608.v1

photocatalysis showed a percent reduction from 27% ~ 100% in the lab-scale experiment. At the pilot-scale, the reduction with photocatalysis efficiency was reported to be as low as (-53%, generation) to ~62% (mitigation). This decreased percent reduction could result from increased dust and relative humidity for the pilot-scale testing. This study also showed that VOC reduction by UV-A photocatalysis could be reduced with a short treatment time (and therefore the dose), similar to the results of previous studies. The results highlight the requirement to carefully scale up treatments from controlled lab-scale studies into the pilot-scale, and eventually on-farm.

4.2 Evaluation of TiO_2 coated surfaces with SEM-EDS analysis

We conducted SEM-EDS analyses to gain insight into the morphology and chemical composition of TiO_2 photocatalyst and its interaction with common building materials. The results of analyzed TiO_2 coating morphology on the surface and chemical composition used in this and our previous studies are shown in Table 7. The morphology of coated TiO_2 was different depending on the surface material. TiO_2 sprayed on the glass dried in the form of 'droplets'. The TiO_2 component was detected only on the white 'circle' of dried solid material from evaporated droplets (Table 7 and Figure B.1.a). Therefore, it is predicted that TiO_2 and photocatalysis were most active at those selected fractions of the entire surface. However, for the FRP (fiberglass reinforced plastic used for barn construction), the TiO_2 coating was covering the whole area (Table 7 and Figure B.1.b). The dose of TiO_2 coated on the FRP (embossed part) was the same as the TiO_2 dose coated on the glass (Figure B.2). Interestingly, a large amount of TiO_2 dose was detected in the 'valley' formed between the embossed parts (Figure B.2.c). TiO_2 in the valley formed a thick 'cake', as shown in Figure 7. It is considered likely that the TiO_2 liquid solution was further 'drained' into the valley part of FRP when spraying the solution of TiO_2. It is recommended to conduct trials of TiO2 application on surfaces to learn the spraying technique and control drying conditions to achieve a practically uniform coating.

The dust accumulation on TiO_2 coated surfaces can affect treatment effectiveness. Dust and organic substances were detected on the TiO_2 surface (Table 7). In fact, while most of the dust present on the dust-accumulated TiO_2 sample was removed with canned air spray before analysis, some dust and organic substances attached to the surface were still detected. The accumulated dust is expected to cover the surface with TiO_2 (Figure B.2.b and d). However, the TiO_2 was also detected on the surface of the sample used in an environment where dust accumulated.

Table 7. TiO_2 coating morphology on the sprayed surface of common building materials.

Ref.	TiO_2 Dose	Characteristic	TiO_2 arrangement
[11]	10 μg·cm^{-2}	Coating method: spray TiO_2 coating surface: glass	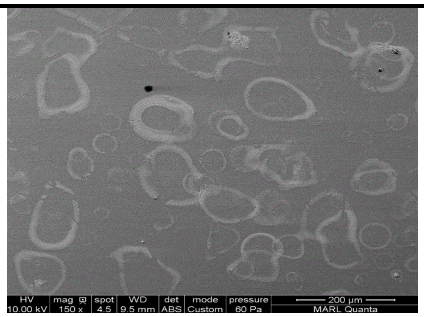
		Coating method: spray TiO_2 coating surface: glass Poultry dust (black) was accumulated for 1 week	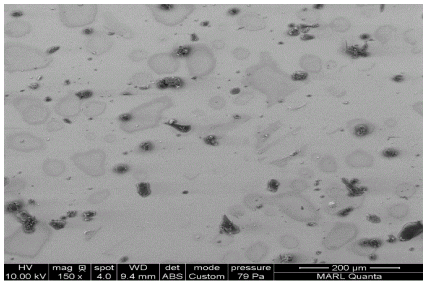

Preprints (www.preprints.org) | NOT PEER-REVIEWED | Posted: 24 December 2020 doi:10.20944/preprints202012.0608.v1

[10]	10 μg·cm^{-2}	Coating method: spray TiO_2 coating surface: FRP Poultry dust (black) was accumulated for 2 month	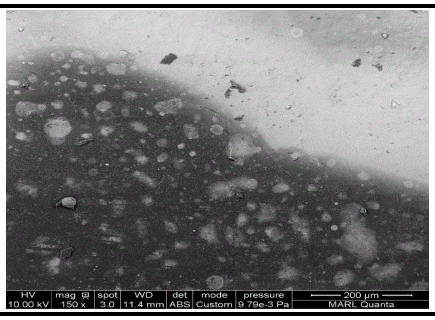
This study	10 μg·cm^{-2}	Coating method: spray TiO_2 coating surface: FRP	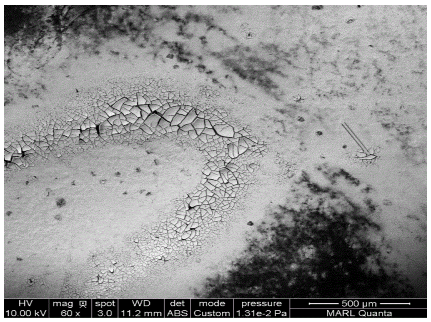

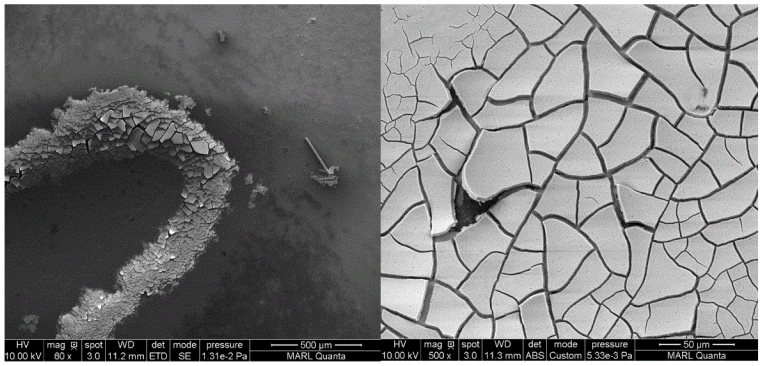

(**a**) (**b**)

Figure 7. Sprayed TiO_2 coating arrangement in the 'valley' formed between the embossed fiberglass reinforced plastic (FRP). (a): 500 μm & (b): 50 μm magnification.

Chemical composition associated with TiO_2 coating was presented in Figure B.2. We observed that the TiO_2 coated on a glass surface was completely removed with propan-2-ol (isopropyl alcohol, Figure B.2.e). Therefore, it is considered that care must be taken when cleaning the TiO_2 coated surface. However, based on the fact that TiO_2 was detected on the surface after photocatalysis in the TIO_2 sample used at 60% relative humidity, it is believed that TiO_2 can operate under high humidity conditions for an extended period of time. However, it is considered that additional experiments are required to test the practical application of TiO_2 coating inside farms where power-washing with water (and sometimes with disinfectants) is performed periodically or in environments where condensation is formed on the wall & ceiling due to temperature differences inside and outside.

5. Conclusions

We designed, tested, and commissioned a mobile laboratory for on-farm research and demonstration of UV treatment for gaseous emissions in real farm conditions. The mobile lab is capable of treating up to 1.2 m^3·s^{-1} of air with TiO_2-based photocatalysis and adjustable UV-A dose based on LED lamps. The commissioning of all systems with standard gases resulted in ~9% and 34% reduction of NH_3 and butan-1-ol, respectively. We demonstrated that as the percent reduction of standard gases increased with increased UV dose by both increased light intensity and treatment

Preprints (www.preprints.org) | NOT PEER-REVIEWED | Posted: 24 December 2020 doi:10.20944/preprints202012.0608.v1

time. The environmental conditions of air flowrate, light intensity, standard gas blending were reproducible. The estimation of extrapolated costs of mitigating targeted gases was possible. The TiO_2 coating was adhering to common building materials, but the overall coating integrity and practical re-application should be investigated in farm-scale trials.

Supplementary Materials: The following are available online at www.mdpi.com/xxx/s1, Figure S.1 -S.18, Table S.1 – S.9.

Author Contributions: conceptualization, J.K., W.J., & H.A.; methodology, J.K.; validation, M.L., W.M., & J.K.; formal analysis, M.L., W.M.; investigation, M.L., W.M., B.F., R.S., B.C., P.L., & C.B.; resources, M.L., W.M., B.F., R.S., BC, P.L., C.B., L.W., and J.K.; data curation, M.L., W.M., & J.K.; writing—original draft preparation, M.L.; writing—review and editing, M.L., W.M., L.W., J.K., & W.J.; visualization, M.L.; supervision, J.K.; project administration, J.K., W.J.; funding acquisition, J.K., W.J.

Funding: This research was supported by Iowa Pork Producers Association Project #18-089 "Employing environmental mitigation technology and/or practices: Treating swine odor and improving air quality with black light." In addition, this research was partially supported by the Iowa Agriculture and Home Economics Experiment Station, Ames, Iowa. Project no. IOW05556 (Future Challenges in Animal Production Systems: Seeking Solutions through Focused Facilitation) sponsored by Hatch Act and State of Iowa funds.

Acknowledgments: The authors gratefully acknowledge Dr. Steven Hoff (ISU) for his help with the construction of the mobile laboratory, Woosang Lee (Smart Control & Sensing Inc.) for his help with the gas monitoring system, Bikash Rajkarnikar (PureTi) for coating with a photocatalyst, Jason Gravenhof (SATA) for training with Minijet spraying, Dr. Brett Ramirez & Smith Benjamin (ISU) for helping the installation & calibration of fans, and Warren Straszheim and Jing Dapeng (MARL, ISU) for their help with SEM-EDS analyses.

Conflicts of Interest: The authors do not declare a conflict of interest. The funders did not play any role in the study design, data collection, analysis, interpretation, and decision to write a manuscript or present results.

Appendix A. Images illustrating details of the mobile laboratory setup

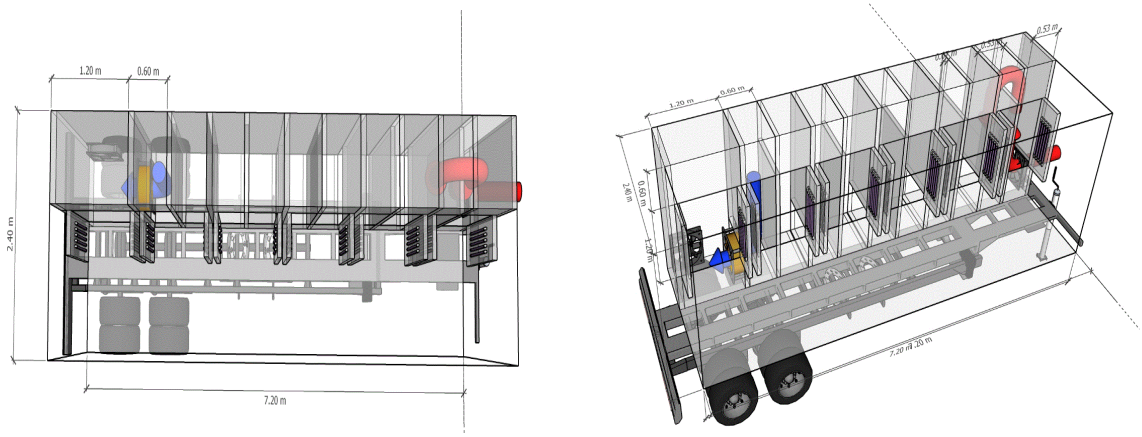

(a) (b)

Figure A.1. Schematic of a flow-through mobile laboratory for UV treatment of gaseous emissions. (a) top view, (b) side view;

Preprints (www.preprints.org) | NOT PEER-REVIEWED | Posted: 24 December 2020 doi:10.20944/preprints202012.0608.v1

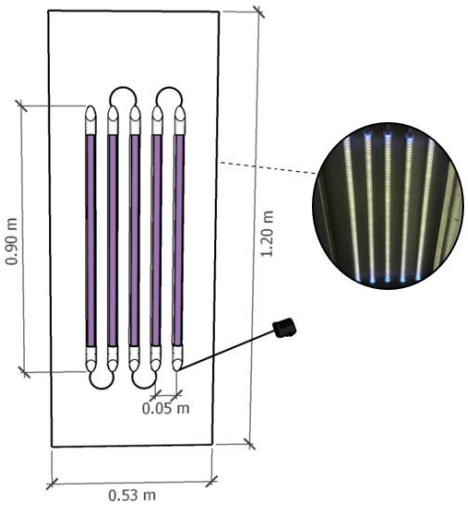

Figure A.2. Schematic of UV-A lamps installation in the treatment chamber.

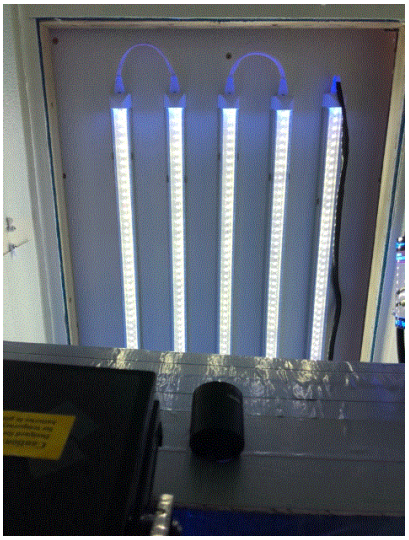

Figure A.3. Picture of measurement of light intensity inside the chamber in the mobile laboratory.

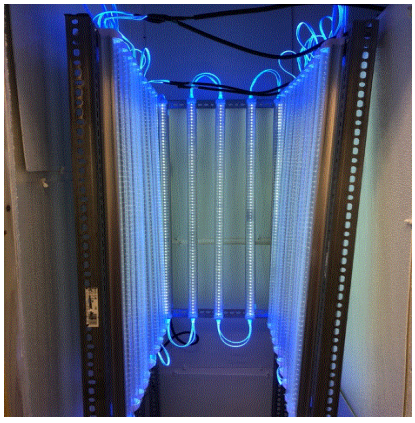

Figure A.4. Picture of additional portable UV-A lamps installed inside Chamber #2 to densify light intensity.

Preprints (www.preprints.org) | NOT PEER-REVIEWED | Posted: 24 December 2020 doi:10.20944/preprints202012.0608.v1

Figure A.5. Picture of the inside of the MERV filtration unit.

Figure A.6. Picture of UV mobile laboratory (back) and filter house mounted on a trailer (front) during the preparatory construction phase.

Figure A.7. Picture of UV mobile laboratory work area. UV treatment area is behind the sealed doors to the right.

Preprints (www.preprints.org) | NOT PEER-REVIEWED | Posted: 24 December 2020 doi:10.20944/preprints202012.0608.v1

Appendix B. Images of photocatalyst on common building surfaces (SEM-EDS analysis)

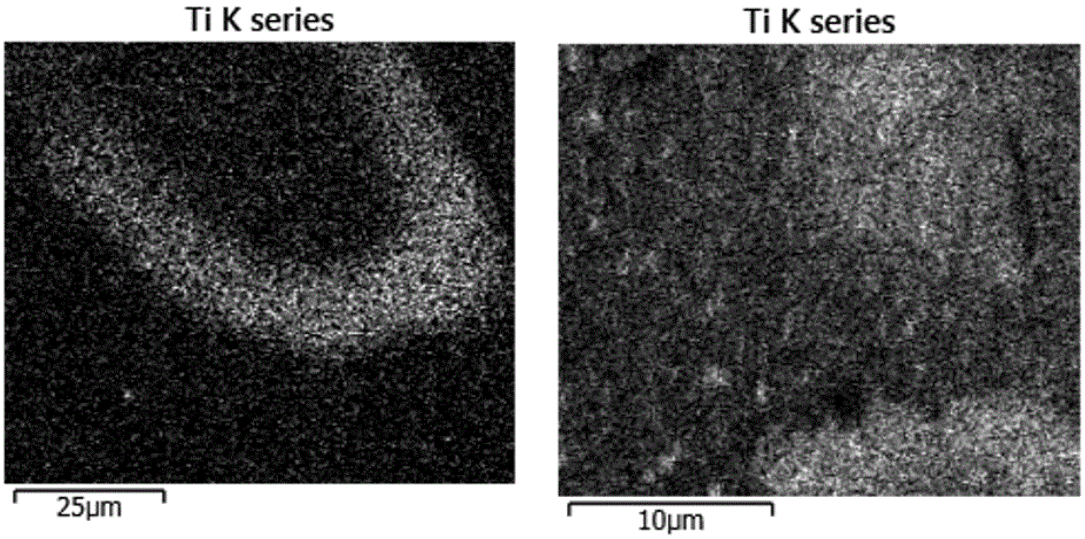

(a) (b)

Figure B.1. Map of TiO_2 arrangement detected on the surface. White dots represent detected TiO_2 coating. (a) glass surface, (b) fiberglass reinforced plastic (FRP) surface;

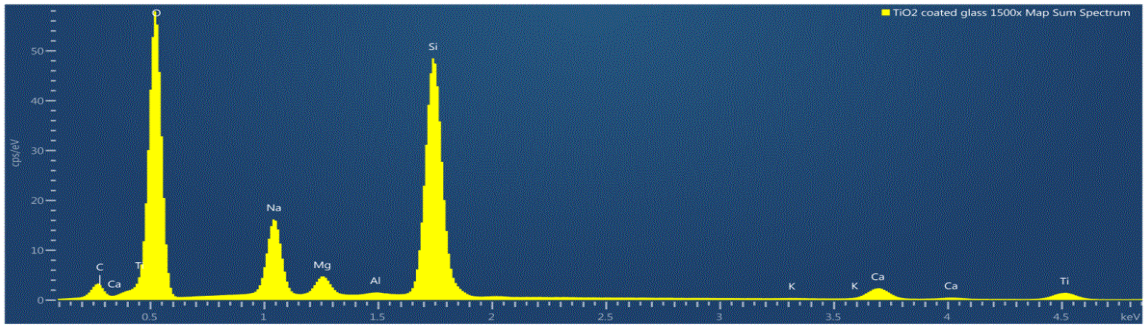

(a)

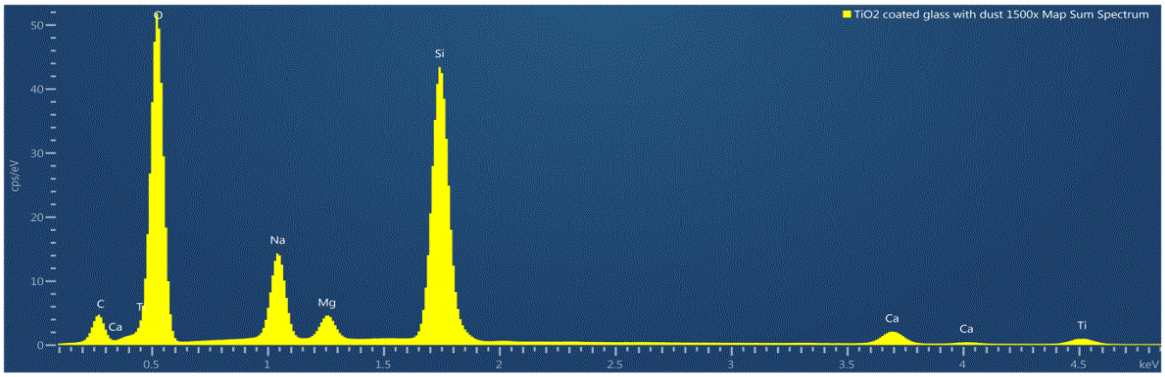

(b)

Preprints (www.preprints.org) | NOT PEER-REVIEWED | Posted: 24 December 2020 doi:10.20944/preprints202012.0608.v1

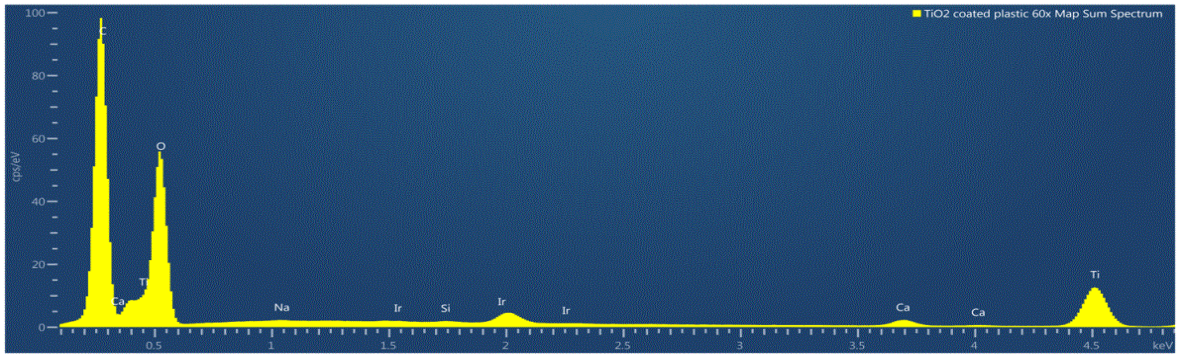

(c)

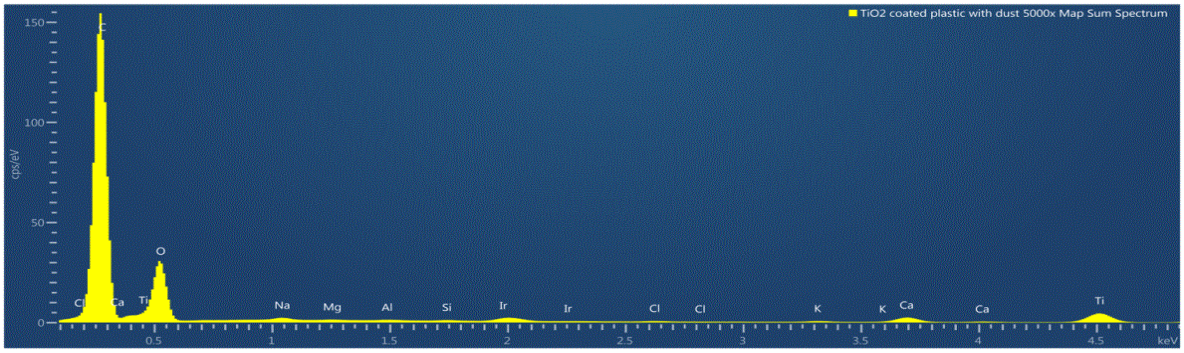

(d)

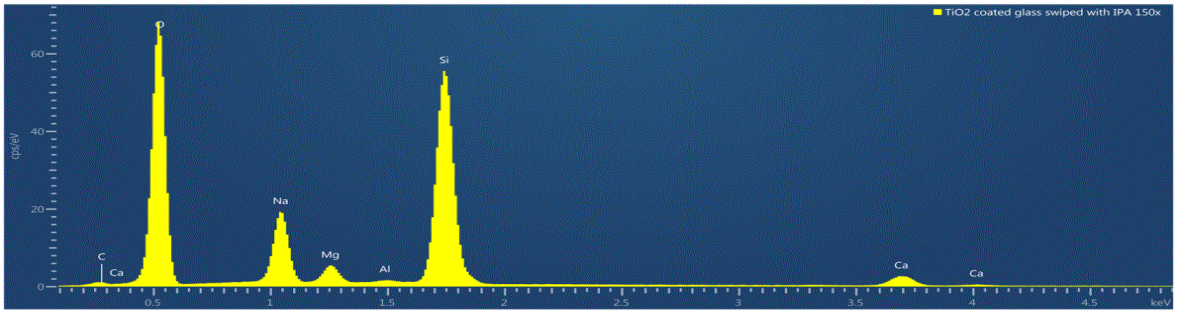

(e)

Figure B.2. Chemical components detected on surfaces of common building materials. (a): glass, (b): glass with poultry dust, (c) The 'valley' part of the embossed fiberglass reinforced plastic (FRP) surface, (d): The embossed part of FRP with accumulated poultry dust, (e): glass with propan-1-ol solvent (example of TiO_2 removal from the surface).

References

1. Cai, L.; Koziel, J.A.; Zhang, S.; Heber, A.J.; Cortus, E.L.; Parker, D.B.; Hoff, S.J.; Sun, G.; Heathcote, K.Y.; Jacobson, L.D. Odor and odorous chemical emissions from animal buildings: Part 3. Chemical emissions. *Transactions of the ASABE* **2015**, *58*, 1333-1347. https://doi: 10.13031/trans.58.11199.
2. Heber, A.J.; Bogan, B.W.; Ni, J.-Q.; Lim, T.T.; Ramirez-Dorronsoro, J.C.; Cortus, E.L.; Diehl, C.A.; Hanni, S.M.; Xiao, C.; Casey, K.D. The national air emissions monitoring study: overview of barn sources. In Proceedings of Livestock Environment VIII, Iguassu Falls, Brazil, St. Joseph Michigan: *ASABE* **2008**; p. 28.

3. Akdeniz, N.; Jacobson, L.D.; Hetchler, B.P.; Bereznicki, S.D.; Heber, A.J.; Koziel, J.A.; Cai, L.; Zhang, S.; Parker, D.B. Odor and odorous chemical emissions from animal buildings: Part 2. Odor emissions. *Transactions of the ASABE* **2012**, *55*, 2335-2345. https://doi: 10.13031/2013.42495.
4. Akdeniz, N.; Jacobson, L.D.; Hetchler, B.P.; Bereznicki, S.D.; Heber, A.J.; Koziel, J.A.; Cai, L.; Zhang, S.; Parker, D.B. Odor and odorous chemical emissions from animal buildings: Part 4. Correlations between sensory and chemical measurements. *Transactions of the ASABE* **2012**, *55*, 2347-2356. https://doi: 10.13031/2013.42496.
5. Bereznicki, S.D.; Heber, A.J.; Akdeniz, N.; Jacobson, L.D.; Hetchler, B.P.; Heathcote, K.Y.; Hoff, S.J.; Koziel, J.A.; Cai, L.; Zhang, S. Odor and odorous chemical emissions from animal buildings: Part 1. Project overview, collection methods, and quality control. *Transactions of the ASABE* **2012**, *55*, 2325-2334. https://doi: 10.13031/2013.42497
6. Parker, D.B.; Koziel, J.A.; Cai, L.; Jacobson, L.D.; Akdeniz, N.; Bereznicki, S.; Lim, T.; Caraway, E.; Zhang, S.; Hoff, S. Odor and odorous chemical emissions from animal buildings: Part 6. Odor activity value. *Transactions of the ASABE* **2012**, *55*, 2357-2368. https://doi: 10.13031/2013.42498.
7. Zhang, S.; Koziel, J.A.; Cai, L.; Hoff, S.J.; Heathcote, K.Y.; Chen, L.; Jacobson, L.D.; Akdeniz, N.; Hetchler, B.P.; Parker, D.B. Odor and odorous chemical emissions from animal buildings: Part 5. Simultaneous chemical and sensory analysis with gas chromatography-mass spectrometry-olfactometry. *Transactions of the ASABE* **2015**, *58*, 1349-1359. https://doi: 10.13031/trans.58.11123
8. Maurer, D.L.; Koziel, J.A.; Harmon, J.D.; Hoff, S.J.; Rieck-Hinz, A.M.; Andersen, D.S. Summary of performance data for technologies to control gaseous, odor, and particulate emissions from livestock operations: Air management practices assessment tool (AMPAT). *Data in Brief* **2016**, *7*, 1413-1429. https://doi.org/10.1016/j.dib.2016.03.070.
9. Koziel, J.; Yang, X.; Cutler, T.; Zhang, S.; Zimmerman, J.; Hoff, S.; Jenks, W.; Laor, Y.; Ravid, U.; Armon, R. Mitigation of odor and pathogens from CAFOs with UV/TiO_2: Exploring the cost effectiveness. In Proceedings of Proc. Mitigating Air Emissions from Animal Feeding Operations. Conference Proceedings, Des Moines, IA. Iowa State University; pp. 169-173.
10. Lee, M.; Li, P.; Koziel, J.A.; Ahn, H.; Wi, J.; Chen, B.; Meiirkhanuly, Z.; Banik, C.; Jenks, W. Pilot-scale testing of UV-A light treatment for mitigation of NH_3, H_2S, GHGs, VOCs, odor, and O_3 inside the poultry barn. *Frontiers in Chemistry* **2020**, *8*, 613. https://doi.org/10.3389/fchem.2020.00613.
11. Lee, M.; Wi, J.; Koziel, J.A.; Ahn, H.; Li, P.; Chen, B.; Meiirkhanuly, Z.; Banik, C.; Jenks, W. Effects of UV-A Light Treatment on Ammonia, Hydrogen Sulfide, Greenhouse Gases, and Ozone in Simulated Poultry Barn Conditions. *Atmosphere* **2020**, *11*, 283. https://doi.org/10.3390/atmos11030283.
12. Maurer, D.L.; Koziel, J.A. On-farm pilot-scale testing of black ultraviolet light and photocatalytic coating for mitigation of odor, odorous VOCs, and greenhouse gases. *Chemosphere* **2019**, *221*, 778-784. https://doi.org/10.1016/j.chemosphere.2019.01.086.
13. Rockafellow, E.M.; Koziel, J.A.; Jenks, W.S. Laboratory-scale investigation of UV treatment of ammonia for livestock and poultry barn exhaust applications. *Journal of Environmental Quality* **2012**, *41*, 281-288. https://doi.org/10.2134/jeq2010.0536.
14. Yang, X.; Koziel, J.A.; Laor, Y.; Zhu, W.; van Leeuwen, J.H.; Jenks, W.S.; Hoff, S.J.; Zimmerman, J.; Zhang, S.; Ravid, U. VOC Removal from Manure Gaseous Emissions with UV Photolysis and UV-TiO_2 Photocatalysis. *Catalysts* **2020**, *10*, 607. https://doi.org/10.3390/catal10060607.
15. Yang, X.; Zhu, W.; Koziel, J.A.; Cai, L.; Jenks, W.S.; Laor, Y.; van Leeuwen, J.H.; Hoff, S.J. Improved quantification of livestock associated odorous volatile organic compounds in a standard flow-through

system using solid-phase microextraction and gas chromatography–mass spectrometry. *Journal of Chromatography A* **2015**, *1414*, 31-40. https://doi.org/10.1016/j.chroma.2015.08.034.

16. Zhu, W.; Koziel, J.A.; Maurer, D.L. Mitigation of livestock odors using black light and a new titanium dioxide-based catalyst: Proof-of-concept. *Atmosphere* **2017**, *8*, 103. https://doi.org/10.3390/atmos8060103.
17. Costa, A.; Chiarello, G.L.; Selli, E.; Guarino, M. Effects of TiO_2 based photocatalytic paint on concentrations and emissions of pollutants and on animal performance in a swine weaning unit. *Journal of Environmental Management* **2012**, *96*, 86-90. https://doi.org/10.1016/j.jenvman.2011.08.025.
18. Guarino, M.; Costa, A.; Porro, M. Photocatalytic TiO_2 coating—To reduce ammonia and greenhouse gases concentration and emission from animal husbandries. *Bioresource Technology* **2008**, *99*, 2650-2658. https://doi.org/10.1016/j.biortech.2007.04.025.
19. Liu, Z.; Murphy, P.; Maghirang, R.; DeRouchey, J. Mitigation of air emissions from swine buildings through the photocatalytic technology using UV/TiO_2. *ASABE Annual International Meeting* **2015**; p. 1. https://doi:10.13031/aim.20152189332.
20. Yao, H.; Feilberg, A. Characterisation of photocatalytic degradation of odorous compounds associated with livestock facilities by means of PTR-MS. *Chemical Engineering Journal* **2015**, *277*, 341-351.
21. Handbook, A. Thermal Comfort. ASHRAE Handbook of Fundamentals. Atlanta, GA. *American Society of Heating, Refrigerating and Air Conditioning Engineers* **2013**. https://doi.org/10.1016/j.cej.2015.04.094.
22. Hoff, S.J.; Bundy, D.S.; Nelson, M.A.; Zelle, B.C.; Jacobson, L.D.; Heber, A.J.; Ni, J.; Zhang, Y.; Koziel, J.A.; Beasley, D.B. Real-time airflow rate measurements from mechanically ventilated animal buildings. *Journal of the Air & Waste Management Association* **2009**, *59*, 683-694. https://doi.org/10.3155/1047-3289.59.6.683.
23. EIA. Energy information administration. *Energy Information Administration Iowa: State Profile and Energy Estimates* **2018**.